

Critical behavior at nematic–smectic- A_1 phase transitions. II. Preasymptotic three-dimensional XY analysis of x-ray and C_p data

C. W. Garland and G. Nounesis*

Center for Materials Science and Engineering and Department of Chemistry, Massachusetts Institute of Technology, Cambridge, Massachusetts 02139

M. J. Young and R. J. Birgeneau

Center for Materials Science and Engineering and Department of Physics, Massachusetts Institute of Technology, Cambridge, Massachusetts 02139

(Received 18 June 1992)

X-ray data are reported for the nematic phase near the nematic (N)–smectic- A_1 ($Sm-A_1$) transition in a binary mixture of pentyphenylcyanobenzoyloxy benzoate (DB_5CN) + cyanobenzoyloxy-pentylstilbene (C_5 stilbene). These data and x-ray data from four other N – $Sm-A_1$ systems, plus the corresponding high-resolution C_p data, are analyzed using the exact solutions of preasymptotic three-dimensional (3D) XY theory. The correlation volume $\xi_{\parallel}\xi_{\perp}^2$, smectic susceptibility σ , and heat capacity C_p are in good agreement with preasymptotic theoretical predictions. First-order corrections-to-scaling terms were known previously to be important for describing C_p ; their importance for $\xi_{\parallel}\xi_{\perp}^2$ and σ is demonstrated here. Many universal features of the 3D XY model are confirmed by the present self-consistent analysis, but the critical anisotropy of the individual lengths ξ_{\parallel} and ξ_{\perp} and the fact that C_p exhibits a normal XY amplitude ratio rather than the theoretically predicted inverted ratio are still unresolved issues.

PACS number(s): 64.70.Md, 61.30.-v, 64.60.Fr

I. INTRODUCTION

The nematic (N)–smectic- A ($Sm-A$) transition in liquid crystals involves the development of a one-dimensional density modulation in an orientationally ordered fluid of long rodlike organic molecules. The critical behavior at second-order N – $Sm-A$ transitions is one of the most challenging unresolved problems in the statistical mechanical theory of phase transitions. Extensive theoretical [1–6] and experimental [7–15] studies of the N – $Sm-A$ transition have been carried out over the past 20 years. The most detailed theoretical treatments predict that this transition belongs to the three-dimensional XY universality class ($d=3, n=2$ vector model), albeit with an inverted C_p amplitude ratio [2,3]. However, there are difficult and not fully resolved issues of Landau-Peierls instability (yielding $d=3$ as the lower marginal dimensionality) [3], coupling of the smectic-order parameter with nematic director fluctuations (implying crossover toward an anisotropic fixed point) [3,6], coupling of the smectic- and the nematic-order parameters (driving the transition first order via a tricritical point) [1], and possible anisotropic corrections-to-scaling terms (not yet considered theoretically).

Experimentally, one must distinguish several $Sm-A$ structures. Nonpolar molecules exhibit only a single type of a smectic- A phase, to be denoted by $Sm-A_m$. Polar molecules, especially those with long aromatic cores and strongly polar head groups, can exhibit smectic- A polymorphism: a monolayer $Sm-A_1$ phase ($d \simeq L$), a partial bilayer $Sm-A_d$ phase ($L < d < 2L$), and a bilayer $Sm-A_2$ phase ($d \simeq 2L$), where d is the layer thickness and L is the molecular length [5]. A wide range of investigations

of N – $Sm-A_m$ and N – $Sm-A_d$ transitions have shown system-dependent nonuniversal critical behavior [7–10]. However, recent calorimetric studies of several N – $Sm-A_1$ transitions [13,14] show that the behavior of C_p is in excellent agreement with orthodox (noninverted) three-dimensional (3D) XY theory, and these C_p data clearly demonstrate the importance of including corrections-to-scaling terms in the analysis of the critical behavior. The nonuniversal behavior observed previously for N – $Sm-A_m$ and N – $Sm-A_d$ transitions [7–10] seems to be related to coupling between smectic and nematic order since the nematic range is small in such systems ($T_{NI} - T_{NA} \leq 40$ K, where I denotes the isotropic phase). As first proposed by de Gennes [1], smectic-nematic coupling can cause a crossover to tricritical and first-order transitions, and this has been observed when the nematic range is sufficiently small [8,9]. In the case of the N – $Sm-A_1$ systems with 3D XY heat-capacity behavior, the nematic range is wide. Thus the nematic order is close to saturated near T_{NA_1} , and smectic-nematic coupling should not play an important role.

In order to establish a global view of N – $Sm-A_1$ critical behavior in the systems exhibiting 3D XY heat capacities, high-resolution x-ray studies are needed to characterize the behavior of the correlation length parallel to the nematic director ξ_{\parallel} , the perpendicular correlation length ξ_{\perp} , and the smectic susceptibility σ . Previous N – $Sm-A_1$ x-ray results are available for mixtures of hexylphenylcyanobenzoyloxy benzoate (DB_6CN) + terephthal-bis-butylaniline (TBBA) [11], for the compounds $T7$ and $T8$ where Tn is alkoxybenzoyloxy-cyano-stilbene [12], and for octyloxyphenylcyanobenzoyloxy benzoate (8OPCBOB) [15]. In the DB_6CN +TBBA sys-

TABLE I. Molecular formulas and nematic range $T_{NI} - T_{NA_1}$. φ denotes $\text{---}\langle\bigcirc\rangle\text{---}$.

System	Nematic range (K)	Formula
T8	189	$\text{C}_8\text{H}_{17}\text{---O---}\varphi\text{---COO---}\varphi\text{---CH=CH---}\varphi\text{---CN}$
T7	167	$\text{C}_7\text{H}_{15}\text{---O---}\varphi\text{---COO---}\varphi\text{---CH=CH---}\varphi\text{---CN}$
DB ₅ CN	120	$\text{C}_5\text{H}_{11}\text{---}\varphi\text{---OOC---}\varphi\text{---OOC---}\varphi\text{---CN}$
+ C ₅ stilbene	($X=0.495$)	$\text{C}_5\text{H}_{11}\text{---}\varphi\text{---CH=CH---}\varphi\text{---OOC---}\varphi\text{---CN}$
DB ₈ ONO ₂	96	$\text{C}_8\text{H}_{17}\text{---O---}\varphi\text{---OOC---}\varphi\text{---OOC---}\varphi\text{---NO}_2$
8OPCBOB	45	$\text{C}_8\text{H}_{17}\text{---O---}\varphi\text{---OOC---}\varphi\text{---O---CH}_2\text{---}\varphi\text{---CN}$

tem, heat-capacity data are lacking, the chemical stability is poor, and the phase diagram is rather complex. T7 and T8 are less stable than 8OPCBOB, but all three of these systems provide results suitable for detailed analysis. We have recently completed a high-resolution calorimetric and x-ray study of the N -Sm- A_1 transition in octyloxyphenylnitrobenzoyloxy benzoate (DB₈ONO₂), and the results are reported in the preceding paper [16] (to be denoted as paper I).

The present paper reports in Sec. II the results of an x-ray study of a mixture of DB₅CN (the pentyl analog of DB₆CN) + C₅ stilbene (cyanobenzoyl-oxypentylstilbene) for which heat-capacity data are already available [13,17]. Thus there are five N -Sm- A_1 systems suitable for detailed analysis: T8, T7, DB₅CN+C₅ stilbene, DB₈ONO₂, 8OPCBOB. For convenience, the molecular formulas of these compounds are given in Table I. Note that they are all typical "frustrated" smectics [5,18] with aromatic cores containing three phenyl rings and strongly polar CN or NO₂ end groups. The nematic range, defined by $T_{NI} - T_{NA_1}$, is very large for four systems and moderately large for 8OPCBOB, as shown in Table I.

In Sec. III, an extensive analysis of the N -Sm- A_1 critical behavior in these five systems is carried out using the exact solutions of preasymptotic 3D XY theory [19-21]. This requires the inclusion of corrections-to-scaling terms, an aspect that has been neglected in all previous analyses of critical x-ray data in liquid-crystal systems. A preliminary report of such an analysis has been given previously for four of these five systems [22]. Section IV summarizes all the universal features of the 3D XY model confirmed by the N -Sm- A_1 data and addresses unresolved difficulties such as the critical anisotropy in the ξ_{\parallel} and ξ_{\perp} behavior and the fact that C_p data show a normal amplitude ratio rather than the predicted inverted ratio.

II. EXPERIMENTAL RESULTS

High-resolution x-ray measurements were made on a DB₅CN + C₅ stilbene mixture with C₅ stilbene mole fraction $X=0.495$, for which the nematic range $T_{NI} - T_{NA_1}$ is 120 K. Both compounds were synthesized and purified at the Centre Recherche Paul Pascal in Bordeaux. Heat-capacity data are available [13,17] on an essentially identical mixture ($X=0.492$) of materials from the same synthetic batches [17]. The details of the x-ray experimental work are essentially the same as those described in paper

I. In contrast to the DB₈ONO₂ system, there is no observable diffuse Sm- A_d scattering at $(0,0,q'_0)$ in the nematic phase of DB₅CN+C₅ stilbene, only a diffuse Sm- A_1 peak at $(0,0,2q_0)$, where $2q_0=2\pi/d$ and d is the Sm- A_1 layer spacing [23]. The temperature-independent value of $2q_0$ is 0.2115 \AA^{-1} , corresponding to $d=29.71 \text{ \AA}$.

The sample was magnetically aligned in the N phase and the resulting mosaic spread determined in the Sm- A_1 phase was small (0.12° half width at half maximum). The transition temperature was determined by the appearance of the mosaicity in the transverse profile. The initial T_c value was found to be 424.302 K, in good agreement with $T_c=424.425 \text{ K}$ obtained from the C_p data [13]. A slow linear drift in the transition temperature, $dT_c/dt = -32 \text{ mK/day}$, was observed over the long period of x-ray data collection. A correction for this drift was made in determining the reduced temperature $\tau=(T-T_c)/T_c$ to be used in subsequent analysis of the critical behavior.

Longitudinal and transverse x-ray scans through $(0,0,2q_0)$ were carried out at 22 fixed temperatures over the range $2 \times 10^{-5} \leq \tau \leq 1.2 \times 10^{-2}$. The scattering profiles (not shown) look very similar to those shown in Fig. 1 of paper I. Both scans at a given T were fit simultaneously with the structure factor $S(\mathbf{q})$ convoluted with the instrumental resolution function. The form used for $S(\mathbf{q})$ was the standard choice discussed in paper I:

$$S(\mathbf{q}) = \sigma / [1 + \xi_{\parallel}^2(q_{\parallel} - 2q_0)^2 + \xi_{\perp}^2 q_{\perp}^2 + c \xi_{\perp}^4 q_{\perp}^4], \quad (1)$$

where the coefficient c of the quartic term is a freely adjustable parameter. Figure 1 shows the dependence of the quantities ξ_{\parallel} , ξ_{\perp} and σ on the reduced temperature τ . As is conventionally done, the critical behavior of these parameters will be described at this point using pure power laws and effective critical exponents:

$$\xi_{\parallel} = \xi_{\parallel 0} \tau^{-\nu_{\parallel}}, \quad \xi_{\perp} = \xi_{\perp 0} \tau^{-\nu_{\perp}}, \quad \sigma = \sigma_0 \tau^{-\gamma}. \quad (2)$$

The least-squares values of these fitting parameters are given in Table II, where for later convenience we also give the parameters for a fit to the correlation volume $\xi_{\parallel} \xi_{\perp}^2$ using

$$\xi_{\parallel} \xi_{\perp}^2 = (\xi_{\parallel} \xi_{\perp}^2)_0 \tau^{-3\nu_{\text{eff}}}. \quad (3)$$

Note that $\gamma \approx \gamma_{XY} = 1.316$ but $\nu_{\parallel} > \nu_{XY} > \nu_{\perp}$, where $\nu_{XY} = 0.669$. Also $\Delta\nu = \nu_{\parallel} - \nu_{\perp} = 0.16 \pm 0.03$ is comparable to the anisotropy in other N -Sm- A systems [7].

The variations of the quartic term coefficient c and the

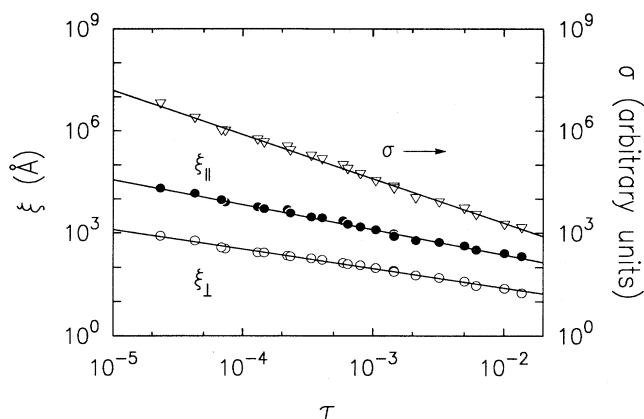


FIG. 1. The dependence on the reduced temperature τ of the smectic- A_1 susceptibility σ in arbitrary units and the correlation lengths ξ_{\parallel} and ξ_{\perp} , as obtained from fitting the x-ray profiles with Eq. (1). The lines represent least-squares fits to these quantities with the pure power-law expressions given in Eqs. (2), and the fitting parameters are given in the first line of Table II. The σ values have been shifted up by a factor of 4 to improve the clarity.

correlation length ratio $\xi_{\parallel}/\xi_{\perp}$ are shown in Fig. 2. The τ dependence of c is essentially the same as that obtained for DB_8ONO_2 (shown in Fig. 3 of paper I) and also that reported for other N -Sm- A systems [10,12]. As discussed in paper I, we have tested three forms for the structure factor $S(\mathbf{q})$: a simple Lorentzian, Eq. (1) with $c=0$; the non-Lorentzian given by Eq. (1); an empirical Lorentzian with a power-law correction, given by Eq. (3) of paper I. The fits to the profiles with Eq. (I-3) are as good as those with Eq. (1), but the Lorentzian fits are clearly poorer. Table II shows that the effective critical exponents obtained using pure power-law fits for ξ_{\parallel} , ξ_{\perp} , and σ values are about the same with all three choices of $S(\mathbf{q})$. Bouwman and de Jeu [15] have proposed an expression for $S(\mathbf{q})$ in which the quartic term in Eq. (1) is replaced by $\xi_s^4 q_{\perp}^4$, where ξ_s is a splay correlation length which is constrained to obey a pure power law near T_c . As shown in paper I for DB_8ONO_2 , Eq. (1) and this Bouwman-de Jeu form yield identical results for ξ_{\perp} . Using the parameters c and ξ_{\perp} from our fit with Eq. (1), we

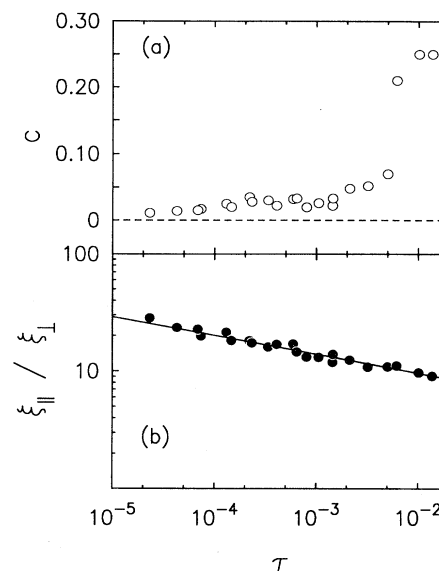


FIG. 2. Reduced temperature dependence of (a) quartic coefficient c obtained when Eq. (1) is used to fit the scattering profile for $\text{DB}_3\text{CN} + \text{C}_5$ stilbene and (b) $\xi_{\parallel}/\xi_{\perp}$ ratio obtained from $S(\mathbf{q})$ fits using Eq. (1) and the c values shown. The best-fit line in (b) has a slope $\Delta\nu = \nu_{\parallel} - \nu_{\perp} = 0.16$.

find that $\xi_s \equiv c^{0.25} \xi_{\perp}$ is well described by $\xi_{s0} \tau^{-\nu_s}$ with $\xi_{s0} = 2.056 \text{ \AA}$ and $\nu_s = 0.46$.

III. PREASYMPTOTIC ANALYSIS

N -Sm- A_1 critical behavior is analyzed below in terms of preasymptotic 3D XY theory that includes corrections-to-scaling terms. Renormalization-group theory [3,19] provides a description of critical singularities in C_p , order-parameter susceptibility χ , and correlation length ξ only in the asymptotic (pure power-law) limit. Heat-capacity studies of liquid-crystal transitions show that it is very difficult to access this asymptotic domain, and correction terms play an important role for C_p analysis over the $10^{-5} < \tau < 10^{-2}$ reduced temperature range [9,13,14]. However, because of the absence of a theory for anisotropic critical behavior, conventional x-

TABLE II. Least-squares $\text{DB}_3\text{CN} + \text{C}_5$ stilbene parameters (with the 95% confidence limits) for pure power-law fits to ξ_{\parallel} , ξ_{\perp} , $\xi_{\parallel}\xi_{\perp}^2$, and σ with Eqs. (2) and (3). The units for $\xi_{\parallel 0}$ and $\xi_{\perp 0}$ are \AA and those for $(\xi_{\parallel}\xi_{\perp}^2)_0$ are \AA^3 . The units of σ_0 are arbitrary. The range of all fits was $2 \times 10^{-5} \leq \tau \leq 1.2 \times 10^{-2}$. The χ^2_{ν} value applies to the $\xi_{\parallel}\xi_{\perp}^2$ fit.

Type of $S(\mathbf{q})$ fit	$\xi_{\parallel 0}$	ν_{\parallel}	$\xi_{\perp 0}$	ν_{\perp}	σ_0	γ	$(\xi_{\parallel}\xi_{\perp}^2)_0$	$3\nu_{\text{eff}}$	χ^2_{ν}
Eq. (1) $c \neq 0$	7.91 ± 0.34	0.73 ± 0.03	1.84 ± 0.08	0.57 ± 0.03	1.22 ± 0.05	1.30 ± 0.05	23.20 ± 1.11	1.88 ± 0.09	1.50
Eq. (1) $c = 0$	10.42 ± 0.70	0.74 ± 0.05	2.37 ± 0.16	0.59 ± 0.04	2.13 ± 0.11	1.32 ± 0.07	59.68 ± 3.69	1.94 ± 0.12	1.73
Eq. (I-3) $\eta_{\perp} \neq 0$	8.56 ± 0.46	0.75 ± 0.04	1.17 ± 0.06	0.59 ± 0.03	1.67 ± 0.09	1.30 ± 0.06	13.32 ± 0.71	1.95 ± 0.10	1.65

ray analysis has neglected correction terms and used pure power laws with adjustable effective critical exponents, a procedure which yields $\nu_{\parallel} > \nu_{\perp}$. We shall argue below that an analysis using corrections-to-scaling terms may nevertheless be used successfully for the correlation volume $\xi_{\parallel} \xi_{\perp}^2$.

Bagnuls and Bervillier [19–21] have carried out an exact nonperturbative analysis of the ϕ^4 field-theory model for three-dimensional n vector models with $n=1,2,3$. They have reported detailed numerical evaluations of the universal aspects of the preasymptotic (first confluent corrections) regime [19] and have tested their predictions for the 3D XY ($d=3, n=2$) model with experimental C_p data for liquid helium near its λ transition [21]. This preasymptotic isotropic theory shows that corrections-to-scaling terms for C_p , correlation length, and susceptibility all depend on a single nonuniversal temperature scaling parameter θ_0 that can be evaluated from the C_p analysis alone. Thus, it is internally inconsistent to ignore correction terms in the x-ray analysis when they are known to be large for C_p . The essential features of preasymptotic 3D XY theory are summarized below, and the theory is then utilized for the analysis of C_p , σ , ξ_{\parallel} , ξ_{\perp} , and the correlation volume $\xi_{\parallel} \xi_{\perp}^2$.

For a scaling analysis of critical behavior there are two dimensionless theoretical scaling fields t^* and h^* :

$$t^* = \theta\tau \text{ and } h^* = \psi H, \quad (4)$$

where τ is the experimental reduced temperature and H is the experimental field conjugate to the order parameter, and one coupling parameter g_0 with the dimension inverse length. The experimental free energy per unit volume $\bar{F}_{\text{expt}}(T)$ is given by

$$\bar{F}_{\text{expt}}(T) = k_B T F_{\text{theor}}(t^*) + \bar{F}_{\text{reg}}(T), \quad (5)$$

where $\bar{F}_{\text{reg}}(T)$ is the regular background contribution and the critical theoretical free energy F_{theor} has the dimensions (volume) $^{-1}$. Taking into account analyticity, one obtains near a critical point

$$t^* = \theta\tau = \theta_0(1 + \theta_1\tau + \dots)\tau, \quad (6)$$

$$g_0 = g_{00}(1 + g_{01}\tau + \dots). \quad (7)$$

Within the preasymptotic critical domain D_{preas} for the ϕ^4 model, θ_0 , ψ , and g_{00} are the only adjustable (nonuniversal system-dependent) parameters and $t^* = \theta_0\tau$, $g_0 = g_{00}$. Higher-order analytic correction terms can arise due to nonzero θ_1 and g_{01} as well as the factor T in Eq. (5) [21]. Bagnuls and Bervillier [19] show that the preasymptotic form for a dimensionless function $f^*(t^*)$, such as $\xi^*(t^*)$, $\chi^*(t^*)$, or $C_p^*(t^*)$, is

$$f^*(t^*) = X_1(t^*)^{-e} [1 + X_2(t^*)^{\Delta_1}]^{X_3} \times [1 + X_4(t^*)^{\Delta_1}]^{X_5} + X_6, \quad (8)$$

where e is the appropriate critical exponent and X_6 is nonzero only for C_p . The corrections-to-scaling exponent $\Delta_1 = 0.524 \pm 0.004$ for a 3D XY model [19], and the values of X_i are well determined numerically in D_{preas} as long as

$t^* = \theta_0\tau < 10^{-2}$. It is usual to expand the expression in Eq. (8) to obtain

$$f^*(t^*) \cong X_1(t^*)^{-e} [1 + (X_2X_3 + X_4X_5)(t^*)^{\Delta_1}] + X_6. \quad (9)$$

Although this approximate form is adequate over the τ range of experimental interest for C_p , it is not sufficiently accurate for ξ and χ due to the large values of X_4^{ξ} and X_4^{χ} [24]. For ξ and χ , one can expand only the term $[1 + X_2(t^*)^{\Delta_1}]^{X_3}$ in Eq. (8).

Presented below is an analysis of C_p and the x-ray data for five liquid-crystal systems exhibiting well-characterized N -Sm- A_1 transitions: DB₈ONO₂ (paper I), DB₅CN + C₅ stilbene (present paper and Ref. [17]), 8OPCBBOB (Refs. [13] and [15]), T7 (Ref. [12]), and T8 (Ref. [12]). The heat capacity will be analyzed first in order to determine the value of θ_0 . This value will then be used in the analysis of the x-ray data.

A. Heat-capacity analysis

This section presents a reanalysis of previously published C_p data using nonasymptotic XY theory. The theoretical 3D XY value of the critical exponent for C_p is $\alpha = -0.0066 \pm 0.0030$ [19], and the nonasymptotic expression for the critical heat capacity above T_c per unit volume $\Delta \bar{C}_p$ is given by

$$\frac{\Delta \bar{C}_p}{k_B} = g_{00}^3 \theta_0^2 \{ X_1^C (\theta_0\tau)^{-\alpha} [1 + (X_2^C X_3^C + X_4^C X_5^C) \times (\theta_0\tau)^{\Delta_1} + D_{2\text{eff}}^+ \tau] + X_6^C \}, \quad (10)$$

where $X_1^C = -118$, $(X_2^C X_3^C + X_4^C X_5^C) = -0.461$, $X_6^C = 112.7$, and $\Delta_1 = 0.524$ [19]. $\Delta \bar{C}_p / k_B = \rho \Delta C_p / k_B$, where ρ is the mass density and the excess heat capacity ΔC_p in J K $^{-1}$ g $^{-1}$ units is given by

$$\Delta C_p = C_p(\text{obs.}) - C_p(\text{background}) = C_p(\text{obs.}) - [B_r + E(T - T_c)]. \quad (11)$$

The usual expression for ΔC_p^{\pm} , where the superscripts denote above and below T_c , is

$$\Delta C_p^{\pm} = A^{\pm} \tau^{-\alpha} [1 + D_1^{\pm} \tau^{\Delta_1} + D_{2\text{eff}}^{\pm} \tau] + B_c, \quad (12)$$

from which it follows that

$$A^+ = -118 g_{00}^3 \theta_0^{2.0066} (k_B / \rho), \quad (13a)$$

$$B_c = 112.7 g_{00}^3 \theta_0^2 (k_B / \rho), \quad (13b)$$

and

$$D_1^+ = -0.461 \theta_0^{0.524}. \quad (14)$$

The correction term $D_{2\text{eff}}\tau$ represents a combination of several higher-order terms that have almost the same τ dependence:

$$D_{2\text{eff}}^+ \tau \cong d_2^C (\theta_0\tau)^{2\Delta_1} + A_1 \tau - \left| \frac{X_6^C \theta_0^\alpha}{X_1^C} \right| A_2 \tau^{1+\alpha}, \quad (15)$$

where the analytic correction terms have coefficients A_1 and A_2 that are functions of α , θ_1 , and g_{01} [21]. Previous analysis of $C_p(N A_1)$ with Eq. (12) using slightly different α and Δ_1 values [13] shows that the $D_{2\text{eff}}^+ \tau$ term becomes important for $\tau > 5 \times 10^{-3}$ or, as we shall see, $t^* = \theta_0 \tau \approx 2 \times 10^{-3}$ typically. It should be noted that setting $D_{2\text{eff}}^+ = 0$ has only a small effect on the other parameters, primarily influencing the D_1^- / D_1^+ ratio [13].

Figure 3 presents the temperature variation of the excess heat capacity ΔC_p for all five systems and shows the quality of the fits to these data with Eq. (12). The fitting parameters obtained when α and Δ_1 are held fixed at the theoretical 3D XY values are given in Table III. It is clear from Fig. 3 and the χ^2_ν values in Table III that the fits are of good quality. The amplitude ratios A^- / A^+ are in good agreement with the 3D XY universal theoretical value $A^- / A^+ = 0.9714 \pm 0.0126$ [20] and are *inconsistent* with an inverted XY value of 1.0294 (see Ref. 13 for a detailed discussion of this point). The ratios D_1^- / D_1^+ are close to +1, the theoretically expected value [25]. A further test of the universality of the C_p fitting parameters is the dimensionless ratio $R_{B_c}^+$ defined by

$$R_{B_c}^+ \equiv A^+ |D_1^+|^{\alpha/\Delta_1} B_c^{-1}, \quad (16)$$

which has the 3D XY value -1.057 ± 0.022 [19]. The $R_{B_c}^+$ values given in Table III are in excellent agreement with this universal theoretical value. Note that for the preasymptotic domain, where $D_{2\text{eff}}^+ \tau$ is not important, there are three fitting parameters for $T > T_c$. The universal ratio $R_{B_c}^+$ could be used to reduce these to two independent variables, in agreement with the presence of two nonuniversal quantities g_{00} and θ_0 in Eq. (10).

Finally, we have used Eq. (14) to determine the θ_0 values, and these are also given in Table III. The uncertainties in θ_0 values have been estimated by stepping θ_0 through a set of values and using the F test. Since the C_p data above T_c are of poorer quality for T7 and T8, these θ_0 values are more uncertain. The value of θ_0 is especially ill-defined for T7, where C_p data extend only 0.7 K above T_c . We have chosen $\theta_0 = 0.23$, in part because of its internal consistency with the x-ray data analysis reported below.

With values established for θ_0 , we can demonstrate the role of the first corrections-to-scaling term (and the $D_{2\text{eff}}^+ \tau$ term) for C_p . Shown in Fig. 4 is a scaling plot of $|(\Delta C_p / k_B g_{00}^3 \theta_0^2) - X_6^C| \equiv |(\Delta C_p^+ - B_c) X_1^C / A^+ \theta_0^\alpha|$ versus the scaling field $\theta_0 \tau$. The solid line represents the preasymptotic 3D XY expression, i.e., Eq. (10) with $D_{2\text{eff}}^+ = 0$. The dashed line is the asymptotic pure power law $|X_1^C| (\theta_0 \tau)^{-\alpha} = 118 (\theta_0 \tau)^{+0.0066}$. Figure 4 shows that the first-order correction term is important for $\theta_0 \tau > 5 \times 10^{-6}$. Note that almost all the liquid-crystal data lie at $\theta_0 \tau$ values greater than this. The upper bound on the preasymptotic domain D_{preas} for C_p corresponds to the $\theta_0 \tau$ value at which the higher-order correction term $D_{2\text{eff}}^+ \tau$ becomes important (see Fig. 4 of Ref. [19]). Since $D_{2\text{eff}}^+ \tau$ is an extra nonuniversal term (not a function

of $\theta_0 \tau$ alone), this bound on D_{preas} will vary with the system. As a typical example, the curve generated using the $\text{DB}_5\text{CN} + \text{C}_5$ stilbene value $D_{2\text{eff}}^+ = 0.87$ is also shown in Fig. 4. For this system, D_{preas} ends around $\theta_0 \tau \approx 2 \times 10^{-3}$.

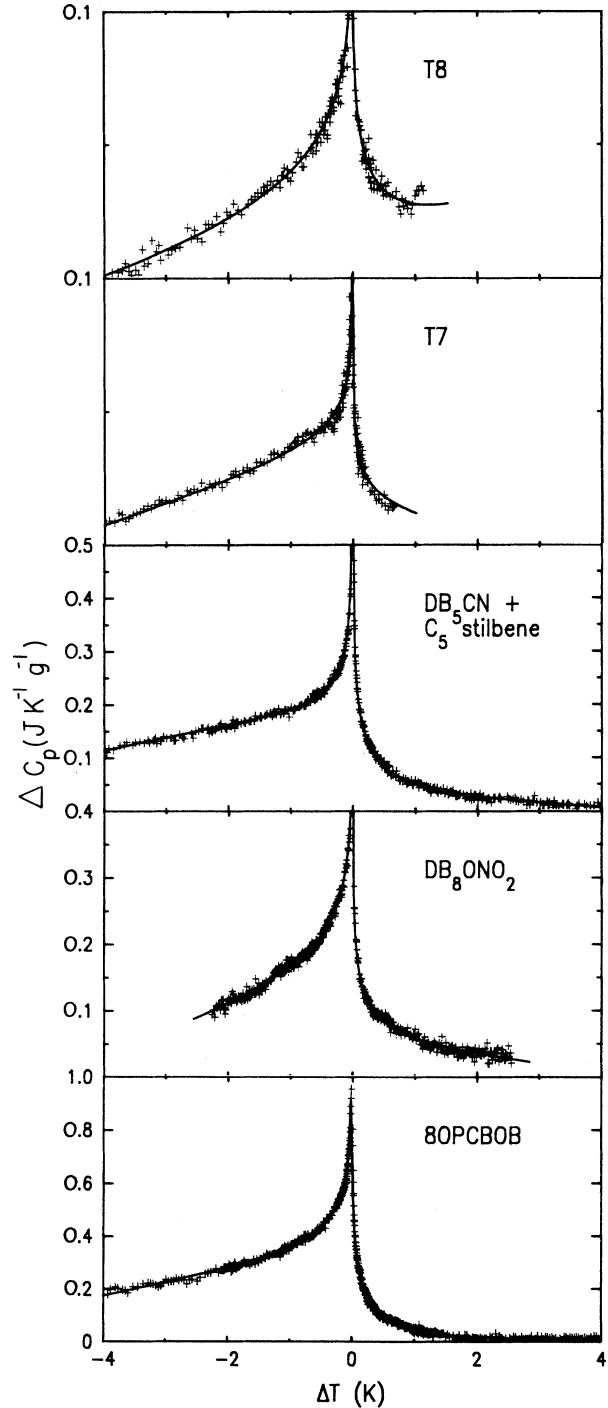


FIG. 3. Excess heat capacity ΔC_p near the N -Sm- A_1 transition in five liquid-crystal systems. Note the use of different ΔC_p scales. The maximum reduced temperature range for the fits with Eq. (12) is $\pm 10^{-2}$; fitting parameters are given in Table III.

TABLE III. Least-squares values of the adjustable parameters (with their 95% confidence limits) for fitting ΔC_p with Eq. (12). For C_p (background), $E=0$ for all fits and B_p ($\text{JK}^{-1}\text{g}^{-1}$) = 2.93 (T8), 2.53 (T7), 2.00 ($\text{DB}_5\text{CN} + \text{C}_5$ stilbene), 2.05 (DB_8ONO_2), and 1.75 (8OPCBOB). $\alpha = \alpha_{XY} = -0.0066$ and $\Delta_1 = \Delta_{XY} = 0.524$ were held fixed. The units for A^+ and B_c are $\text{JK}^{-1}\text{g}^{-1}$.

System	T_c (K)	A^+	A^-/A^+	D_1^+	D_1^-/D_1^+	$D_{2\text{eff}}^+$	$\frac{D_{2\text{eff}}^-}{D_{2\text{eff}}^+}$	B_c	χ_v^2	$R_{B_c}^+$	θ_0
T8	367.170 ± 0.003	-3.34 ± 0.20	0.990 ± 0.004	-0.06 ± 0.10	[1]	-1.56 ± 4.0	-0.49 ± 1.0	3.20 ± 0.20	0.99	-1.076 ± 0.064	0.02 ± 0.03
T7	401.87 ± 0.003	-1.93 ± 0.24	0.983 ± 0.004	-0.21 ± 0.4	0.74 ± 1.5	1.51 ± 4.0	1.25 ± 3.0	1.86 ± 0.24	1.09	-1.058 ± 0.064	0.23 ± 0.50
DB_5CN + C_5 stilbene	424.426 ± 0.001	-18.59 ± 0.23	0.994 ± 0.003	-0.288 ± 0.05	1.32 ± 0.20	0.87 ± 0.13	2.02 ± 0.30	17.74 ± 0.24	0.96	-1.064 ± 0.029	0.41 ± 0.06
DB_8ONO_2	404.351 ± 0.001	-13.19 ± 0.17	0.986 ± 0.003	-0.314 ± 0.07	0.69 ± 0.17	1.27 ± 0.32	1.26 ± 0.32	12.61 ± 0.17	0.94	-1.062 ± 0.027	0.48 ± 0.11
8OPCBOB	394.661 ± 0.001	-31.45 ± 0.41	0.988 ± 0.003	-0.282 ± 0.04	1.01 ± 0.15	0.69 ± 0.10	1.96 ± 0.29	29.95 ± 0.40	0.83	-1.067 ± 0.030	0.39 ± 0.06

It should be noted that the magnitude of θ_0 is relatively large in these polar liquid crystals compared to the value in helium near its normal-superfluid transition. An analysis of helium C_p data in Ref. [20] yields $\theta_0 = 0.015 - 0.016$.

B. X-ray analysis

The theoretical 3D XY values of the correlation length critical exponent ν and the susceptibility critical exponent γ are $\nu = 0.6689 \pm 0.0010$ and $\gamma = 1.3160 \pm 0.0020$ [19]. The nonasymptotic expressions for ξ and χ [also

the intensity σ from Eq. (1), which is proportional to χ] are

$$\xi = g_{00}^{-1} X_1^\xi (\theta_0 \tau)^{-\nu} [1 + X_2^\xi X_3^\xi (\theta_0 \tau)^{\Delta_1} + D_2^\xi \tau] \times [1 + X_4^\xi (\theta_0 \tau)^{\Delta_1}]^{X_5^\xi}, \quad (17)$$

$$\xi = \xi_0 \tau^{-\nu} [1 + 0.3754 (\theta_0 \tau)^{\Delta_1} + D_2^\xi \tau] \times [1 + 29.76 (\theta_0 \tau)^{\Delta_1}]^{0.232}, \quad (18)$$

and

$$\chi = g_{00}^3 \psi^2 X_1^\chi (\theta_0 \tau)^{-\gamma} [1 + X_2^\chi X_3^\chi (\theta_0 \tau)^{\Delta_1} + D_2^\chi \tau] \times [1 + X_4^\chi (\theta_0 \tau)^{\Delta_1}]^{X_5^\chi}, \quad (19)$$

$$\sigma = \sigma_0 \tau^{-\gamma} [1 + 0.5119 (\theta_0 \tau)^{\Delta_1} + D_2^\chi \tau] \times [1 + 24.55 (\theta_0 \tau)^{\Delta_1}]^{0.460}, \quad (20)$$

where $\Delta_1 = 0.524$ as before, $X_1^\xi = 0.392$ and $X_1^\chi = 0.185$, and g_{00} and ψ are system-dependent nonuniversal amplitudes [19]. The nonuniversal parameter θ_0 will be held fixed at the value determined above from fits to C_p . The higher-order correction terms $D_2^\xi \tau$ and $D_2^\chi \tau$ represent a combination of second corrections-to-scaling terms ($\sim \tau^{2\Delta_1} = \tau^{1.048}$) and analytic correction terms ($\sim \tau$):

$$D_2^\xi \tau \approx d_2^\xi (\theta_0 \tau)^{2\Delta_1} - (\nu \theta_1 + g_{01}) \tau, \quad (21a)$$

$$D_2^\chi \tau \approx d_2^\chi (\theta_0 \tau)^{2\Delta_1} - (\gamma \theta_1 - 3g_{01}) \tau. \quad (21b)$$

Both of these terms should be negligible in the preasymptotic domain D_{preas} , and they are retained in Eqs. (17)–(20) for completeness.

An excellent way of visualizing the important role of first-order corrections-to-scaling terms is to display the variation of *effective exponents* ν_{eff} and γ_{eff} defined by $\nu_{\text{eff}} \equiv -d \ln \xi / d \ln(\theta_0 \tau)$ and $\gamma_{\text{eff}} \equiv -d \ln \chi / d \ln(\theta_0 \tau)$ and obtainable from Eqs. (17)–(20) with $D_2^\xi = D_2^\chi = 0$. The resulting values shown in Fig. 5 are valid for $t^* = \theta_0 \tau \leq 10^{-2}$, the limit of the Bagnuls-Bervillier numerical evaluation of X_i values, or to the limit of the preasymptotic domain D_{preas} , which is estimated to lie at a smaller $\theta_0 \tau$ value of about 2×10^{-3} . In any event, it is

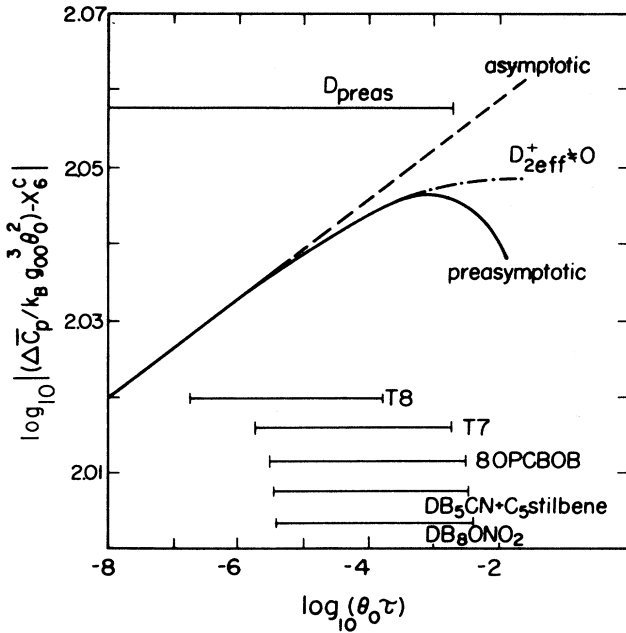


FIG. 4. Scaling plot of $|(\Delta C_p / k_B g_{00}^3 \theta_0^2) - X_6^C|$ vs $\theta_0 \tau$. The solid line is the preasymptotic ($D_{2\text{eff}}^+ = 0$) expression given by Eq. (10), and the dashed line is the asymptotic pure power law. The dash-dotted line is the nonuniversal curve for $\text{DB}_5\text{CN} + \text{C}_5$ stilbene with $D_{2\text{eff}}^+ = 0.87$. The ranges $\theta_0 \tau$ of available C_p data for five liquid-crystal systems are also shown.

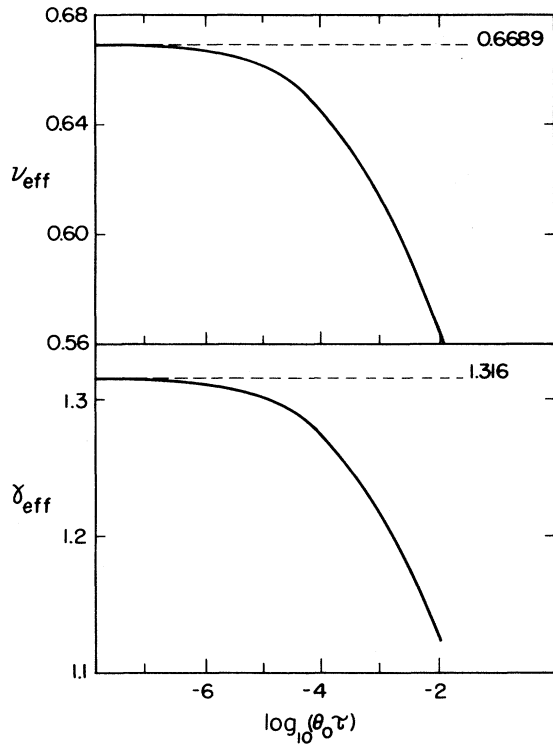


FIG. 5. Effective critical exponents ν_{eff} and γ_{eff} representing ξ and χ . The true asymptotic 3D XY values are given by the horizontal dashed lines. The dependence of ν_{eff} and γ_{eff} on the scaling field $t^* = \theta_0 \tau$ is due to first-order corrections-to-scaling terms.

clear that the liquid-crystal data lie in a $\theta_0 \tau$ range outside the limiting asymptotic regime.

Since pure power-law fits to N -Sm- A_1 x-ray data yield experimental effective exponents $\nu_{\parallel} > \nu_{XY} > \nu_{\perp}$ as shown in Table IV, it is obviously difficult to apply isotropic theory to the correlation lengths. Table IV also shows that preasymptotic (i.e., $D_{\xi}^{\xi} \equiv 0$) fits are quite poor for both ξ_{\parallel} and ξ_{\perp} when θ_0 is held fixed at the value obtained from the heat capacity. This is especially true for the

more anisotropic systems. One might speculate that the experimental anisotropy is completely due to large anisotropic second-order terms $D_{\xi}^{\xi} \tau$, and we have tested empirical fits with θ_0 fixed by the C_p data and $D_{\xi}^{\xi} \neq 0$ as an independent adjustable parameter for ξ_{\parallel} and ξ_{\perp} . Except for 8OPCBOB, there is no significant improvement in the ξ_{\perp} fits and only a modest improvement in the ξ_{\parallel} fits. For 8OPCBOB we find $D_{\xi_{\parallel}}^{\xi} = -69$ ($\chi_v^2 = 1.98$) and $D_{\xi_{\perp}}^{\xi} = 136$ ($\chi_v^2 = 2.3$), but those D_{ξ}^{ξ} values seem physically questionable and the χ_v^2 values are still much worse than those for pure power-law fits. Another empirical fit was to hold $D_{\xi}^{\xi} = 0$ but allow θ_0 to be freely adjustable. The results were not encouraging for ξ_{\parallel} ($\theta_0^{\Delta 1} \rightarrow$ nonphysical negative values) or ξ_{\perp} ($\theta_0^{\Delta 1} \rightarrow$ large values, 11.6 in the case of 8OPCBOB) since the χ_v^2 values were still large. As a final *ad hoc* attempt to represent the experimental anisotropy with Eq. (17), we allowed g_{00} and the coefficient $X_{\xi}^{\xi} X_{\xi}^{\xi}$ to be freely adjustable parameters with $D_{\xi}^{\xi} = 0$ and θ_0 fixed at the C_p value. These two-parameter fits are statistically equivalent to two-parameter pure power fits within 95% confidence limits, but the physical significance of the fitting parameters is unclear [26]. As far as we are aware, the only previous analysis of a quantity related to the correlation length that utilized corrections-to-scaling terms is data fitting for the nematic elastic constant K_3 [27]. This bend constant is given by $K_3 = K_3^0 + \delta K_3$, where δK_3 is expected to vary like ξ_{\parallel} , and fits were made with the form $A \tau^{-\rho_3} (1 + D \tau^{0.5}) + K_3^0$. For three nonpolar N -Sm- A_m systems when D was fixed at zero, $\rho_3 \approx 0.8$ in good agreement with x-ray ν_{\parallel} values. When D is allowed to be a free parameter, $\rho_3 \approx 0.67$ and $D \approx -20$. However, such a large negative D is puzzling since it implies that δK_3 changes sign at $\tau \approx 2.5 \times 10^{-3}$.

In spite of difficulties in analyzing the individual correlation lengths, we believe that one can use the theoretical preasymptotic results for the isotropic 3D XY model to analyze the correlation volume $\xi_{\parallel} \xi_{\perp}^2$ (as well as the smectic susceptibility σ) of liquid crystals near the N -Sm- A_1 transition. The correlation volume is related quite directly to the free energy per unit volume via two-scale-factor universality, as we shall show just below. Thus, it is pos-

TABLE IV. Least-squares values of the adjustable parameters for fits to ξ_{\parallel} and ξ_{\perp} with a pure power law and with Eq. (18). Quantities in brackets were held fixed at the given values. The units for $\xi_{\parallel 0}$ and $\xi_{\perp 0}$ are Å. The range for these fits is $2 \times 10^{-5} < \tau < 1.2 \times 10^{-2}$. The values quoted for T7 and T8 (Ref. [12]), DB₈ONO₂ (Ref. [16]), and 8OPCBOB (Ref. [15]) were obtained from the reanalysis of published data. In the case of 8OPCBOB, our ν_{\perp} value is somewhat smaller than the published value of 0.56 ± 0.05 .

System	$\xi_{\parallel 0}$	ν_{\parallel}	θ_0	χ_v^2	$\xi_{\perp 0}$	ν_{\perp}	θ_0	χ_v^2
T8	14.55	0.699	[0]	0.84	1.49	0.654	[0]	0.84
	17.20	[0.669]	[0.02]	1.26	1.31	[0.669]	[0.02]	0.79
T7	14.83	0.694	[0]	1.37	1.94	0.612	[0]	1.96
	16.24	[0.669]	[0.23]	2.84	1.18	[0.669]	[0.23]	2.21
DB ₅ CN+	7.91	0.732	[0]	1.82	1.84	0.566	[0]	0.89
C ₅ stilbene	10.97	[0.669]	[0.41]	6.33	0.76	[0.669]	[0.41]	3.24
DB ₈ ONO ₂	8.74	0.694	[0]	1.59	1.75	0.593	[0]	1.00
	9.33	[0.669]	[0.48]	3.64	0.89	[0.669]	[0.48]	1.67
8OPCBOB	6.76	0.721	[0]	1.23	1.73	0.547	[0]	1.21
	9.42	[0.669]	[0.39]	5.83	0.545	[0.669]	[0.39]	4.52

sible that $\xi_{\parallel}\xi_{\perp}^2$ may exhibit effectively isotropic behavior even though ξ_{\parallel} and ξ_{\perp} separately are anisotropic (i.e., $\nu_{\parallel} > \nu_{\perp}$). More precise statements are not possible in the absence of a convincing theory for this anisotropy [3,4,6]. The usual statement of two-scale-factor universality is $\bar{F}_{\text{sing}}\xi^3/k_B T = Y$, where \bar{F}_{sing} is the singular free energy per unit volume and Y is a dimensionless universal constant whose value is independent of the system studied in a given universality class [28]. The quantity \bar{F}_{sing} is $k_B T F_{\text{theor}}$ that appears in Eq. (5), and ξ^3 is replaced by $\xi_{\parallel}\xi_{\perp}^2$ in the case of an anisotropic liquid crystal system. Thus,

$$\xi_{\parallel}\xi_{\perp}^2 = Y/F_{\text{theor}}. \quad (22)$$

Note that $F_{\text{theor}} = 0$ at T_c and $F_{\text{theor}} < 0$ for $T > T_c$, which means that Y is a negative number [29]. The value of $F_{\text{theor}}(\tau)$ can be obtained by integrating the preasymptotic XY heat-capacity expression once the nonuniversal fitting parameters g_{00} and θ_0 are known (for which the mass density ρ is required).

Precise values of ρ are not known for the investigated systems, but we can use $\rho = 1.0 \text{ g cm}^{-3}$ with some confidence since several other polar liquid crystals have densities in the range 0.99–1.04 [30]. Figure 6 shows the variation of $\xi_{\parallel}\xi_{\perp}^2$ with τ for DB_8ONO_2 and $\text{DB}_5\text{CN} + \text{C}_5$ stilbene. The line represents Y/F_{theor} , where Y is a temperature-independent adjustable constant. The values of Y were -0.267 for DB_8ONO_2 and -0.285 for $\text{DB}_5\text{CN} + \text{C}_5$ stilbene. Fits of comparable quality were also obtained for $T7$, $T8$, and 8OPCBOB , which yielded $Y = -0.299$ ($T7$), -0.310 ($T8$), and -0.13 (8OPCBOB). Since the C_p variations are well described by the isotropic 3D XY model, the good fits shown in Fig. 6 clearly indicate that the temperature dependence of $\xi_{\parallel}\xi_{\perp}^2$ can be represented empirically by this model.

The nonasymptotic expression for $\xi_{\parallel}\xi_{\perp}^2$ that is a gen-

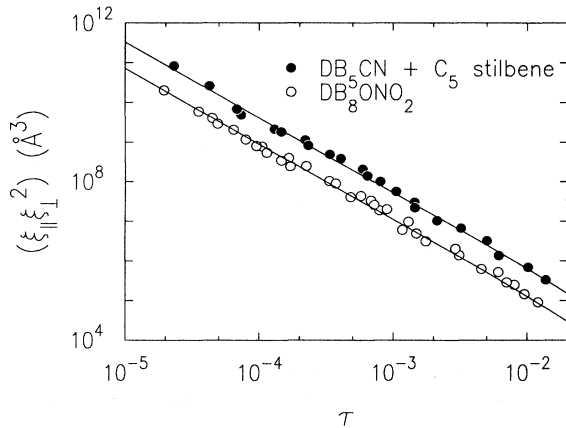


FIG. 6. Temperature dependence of the Sm- A_1 correlation volume $\xi_{\parallel}\xi_{\perp}^2$ for DB_8ONO_2 and $\text{DB}_5\text{CN} + \text{C}_5$ stilbene. The solid fitting line Y/F_{th} has only one adjustable parameter, the temperature-independent constant Y . The data points for the $\text{DB}_5\text{CN} + \text{C}_5$ stilbene mixture have been shifted up by a factor of 5 in order to improve the clarity of the display.

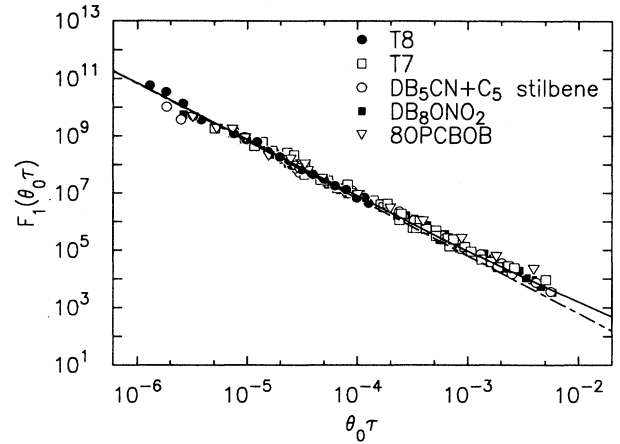


FIG. 7. Scaling plot for the Sm- A_1 correlation volume: $\theta_0\tau$ is the thermal scaling field and $F_1(\theta_0\tau) \equiv \xi_{\parallel}\xi_{\perp}^2/(\xi_{\parallel}\xi_{\perp}^2)_0\theta_0^{3\nu}$. The θ_0 values were determined by C_p fits, see Table III, and used without further adjustment. The solid line represents the preasymptotic 3D XY expression given by Eq. (23). The dashed line is the asymptotic pure power law that will hold sufficiently close to T_c where corrections-to-scaling terms can be neglected.

eralization of Eq. (18) is

$$\xi_{\parallel}\xi_{\perp}^2 = (\xi_{\parallel}\xi_{\perp}^2)_0 \tau^{-3\nu} [1 + 1.126(\theta_0\tau)^{\Delta_1} + D_2^{\nu}\tau] \times [1 + 29.76(\theta_0\tau)^{\Delta_1}]^{0.696}, \quad (23)$$

with $D_2^{\nu} \equiv D_{\parallel}^{\xi} + 2D_{\perp}^{\xi}$ and

$$(\xi_{\parallel}\xi_{\perp}^2)_0 = g_{00}^{-3} (X_{\parallel}^{\xi})^3 \theta_0^{-3\nu} = 0.060 g_{00}^{-3} \theta_0^{-2.0066}. \quad (24)$$

Fits to σ and $\xi_{\parallel}\xi_{\perp}^2$ data have been made with pure power laws, Eqs. (2) and (3), using effective exponents and 3D XY exponents, and with nonasymptotic expressions Eqs. (20) and (23). In the latter case, three variants were test-

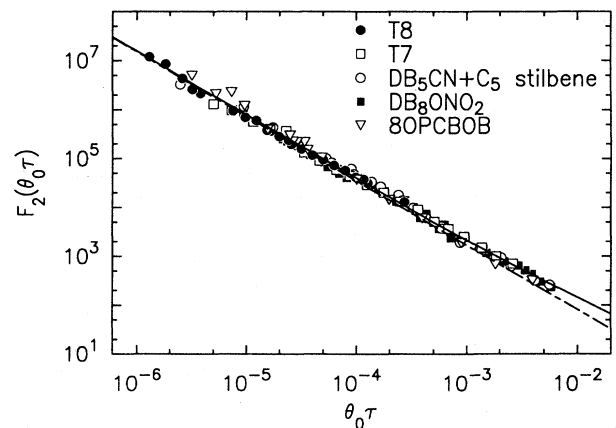


FIG. 8. Scaling plot for the Sm- A_1 susceptibility σ : $\theta_0\tau$ is the scaling field and $F_2(\theta_0\tau) \equiv \sigma/\sigma_0\theta_0^{\nu}$. The θ_0 values are the same as those used in Fig. 7. The solid line represents the preasymptotic 3D XY expression given by Eq. (20), and the dashed line is the asymptotic pure power law.

TABLE V. Least-squares values of the adjustable parameters for fits to $\xi_{\parallel}\xi_1^2$ and σ with Eqs. (23) and (20), respectively. Quantities in brackets were held fixed at the given values. The units for $(\xi_{\parallel}\xi_1^2)_0$ are Å; those for σ_0 are arbitrary. The number of data points N in each fit and the limiting value of F for χ_v^2 (fit 2)/ χ_v^2 (fit 1) at the 95% confidence limit are $N=20, F=2.2$ (T8); $N=39, F=1.7$ (T7); $N=22, F=2.1$ (DB₅CN+C₅ stilbene); $N=33, F=1.8$ (DB₈ONO₂); and $N=17, F=2.4$ (8OPCBOB). The uncertainties for free θ_0 values are 95% confidence limits.

System	Correlation volume					Susceptibility				
	$(\xi_{\parallel}\xi_1^2)_0$	3ν	θ_0	D_2^2	χ_v^2	σ_0	γ	θ_0	D_2^2	χ_v^2
T8	37.99	1.978	[0]	[0]	1.87	0.386	1.262	[0]	[0]	1.32
	31.28	[2.007]	[0]	[0]	1.84	0.267	[1.316]	[0]	[0]	1.66
	28.49	[2.007]	[0.02]	[0]	1.75	0.254	[1.316]	[0.02]	[0]	1.28
	28.71	[2.007]	[0.02]	1.27	1.84	0.239	[1.316]	[0.02]	-22.1	0.96
	29.06	[2.007]	0.013 ±0.028	[0]	1.84	0.231	[1.316]	0.214 ±0.15	[0]	1.08
T7	55.27	1.911	[0]	[0]	1.74	0.648	1.225	[0]	[0]	0.88
	26.56	[2.007]	[0]	[0]	2.19	0.312	[1.316]	[0]	[0]	2.76
	21.45	[2.007]	[0.23]	[0]	1.76	0.281	[1.316]	[0.23]	[0]	1.36
	21.43	[2.007]	[0.23]	-0.17	1.76	0.275	[1.316]	[0.23]	-14.3	1.40
	21.45	[2.007]	0.231 ±0.16	[0]	1.76	0.256	[1.316]	0.925 ±0.51	[0]	1.14
DB ₅ CN +C ₅ stilbene	23.20	1.883	[0]	[0]	1.50	1.22	1.300	[0]	[0]	1.10
	8.64	[2.007]	[0]	[0]	2.93	0.980	[1.316]	[0]	[0]	1.13
	6.74	[2.007]	[0.41]	[0]	1.76	0.825	[1.316]	[0.41]	[0]	1.64
	7.03	[2.007]	[0.41]	5.26	1.72	0.820	[1.316]	[0.41]	14.2	1.31
	6.98	[2.007]	0.308 ±0.21	[0]	1.83	1.07	[1.316]	0.01 ±0.02	[0]	1.05
DB ₈ ONO ₂	26.92	1.872	[0]	[0]	1.71	1.33	1.284	[0]	[0]	1.75
	8.94	[2.007]	[0]	[0]	4.09	0.937	[1.316]	[0]	[0]	2.54
	7.07	[2.007]	[0.48]	[0]	1.98	0.849	[1.316]	[0.48]	[0]	1.56
	7.24	[2.007]	[0.48]	3.67	1.98	0.858	[1.316]	[0.48]	6.51	1.54
	7.04	[2.007]	0.494 ±0.23	[0]	2.04	0.832	[1.316]	0.286 ±0.15	[0]	1.53
8OPCBOB	21.75	1.805	[0]	[0]	1.50	0.187	1.402	[0]	[0]	1.15
	3.05	[2.007]	[0]	[0]	4.93	0.370	[1.316]	[0]	[0]	2.14
	2.98	[2.007]	[0.39]	[0]	3.25	0.316	[1.316]	[0.39]	[0]	4.46
	2.84	[2.007]	[0.39]	-35.1	2.22	0.365	[1.316]	[0.39]	41.3	2.86
	2.33	[2.007]	4.49 ±1.92	[0]	1.52	^a	[1.316]	[0]	[0]	

^aTo achieve a good fit, a *negative* value of $\theta_0^{0.524}$ would be required. Since θ_0 is constrained to be positive, this fit gives a result identical to the $\theta_0=0$ fit.

ed: θ_0 fixed at the C_p value with $D_2=0$, θ_0 fixed with D_2 freely adjustable, and θ_0 freely adjustable with $D_2=0$. The results are compared in Table V. We are most confident about the recent measurements on DB₈ONO₂ and DB₅CN+C₅ stilbene, but the general trends seem to hold for all the systems except perhaps 8OPCBOB. All three variants of the nonasymptotic fits exhibit comparable χ_v^2 values, which is related to the fact that when θ_0 is free its value is reasonably close to the value determined from C_p and when D_2 is allowed to be nonzero its value is small. Furthermore, the preasymptotic fits to $\xi_{\parallel}\xi_1^2$ and σ with θ_0 fixed (and $D_2=0$) are *one-parameter* fits that are statistically equivalent to two-parameter power-law fits within 95% confidence limits, as shown by comparing $\chi_v^2(\text{preas})/\chi_v^2(\text{pure power})$ to the limiting F values given in the caption to Table V. These preasymptotic fits have the great additional advantage of being consistent with 3D

XY theory and high-resolution C_p data.

Figures 7 and 8 display plots of the scaled correlation volume and the scaled smectic susceptibility versus the scaling field $\theta_0\tau$. The quantity shown in Fig. 7 is $F_1(\theta_0\tau) \equiv \xi_{\parallel}\xi_1^2/(\xi_{\parallel}\xi_1^2)_0\theta_0^{3\nu}$, and that shown in Fig. 8 is $F_2(\theta_0\tau) \equiv \sigma/\sigma_0\theta_0^\gamma$. In all five systems, these plots were made using the θ_0 values obtained from the C_p fits. It should be stressed that there is only a single τ -independent adjustable parameter for these plots, the nonuniversal amplitude $(\xi_{\parallel}\xi_1^2)_0$ or σ_0 . The value of $(\xi_{\parallel}\xi_1^2)_0$ is dependent on g_{00} , as shown in Eq. (24); the value of σ_0 depends on both g_{00} and ψ , i.e., $\sigma_0 \propto \chi_0 = g_{00}^3\psi^2X\theta_0^{-\gamma}$, as seen from Eqs. (19) and (20). The quality of the data collapse is fairly good for 8OPCBOB and excellent for the other four systems. One can see from the theoretical curves that first-order corrections-to-scaling terms play a role for $\theta_0\tau \geq 10^{-5}$.

C. Amplitude universality

A final test can be made of the universality of these liquid-crystal C_p and x-ray results. Although the amplitude A^+ for C_p and the amplitude $(\xi_{\parallel}\xi_{\perp}^2)_0$ for the correlation volume are nonuniversal quantities, there is a universal relationship between them. The ratio R_{ξ}^+ is defined in an isotropic system by $(R_{\xi}^+)^3 \equiv \alpha\tau^2(\Delta\bar{C}_p^{\text{ls}}/k_B)(\xi^{\text{ls}})^3$, where the superscript ls denotes the leading singularity. The generalization for an anisotropic system obtained from Eqs. (10)–(12) and (23) is

$$(R_{\xi}^+)^3 = \alpha\tau^2(\rho A^+/k_B)\tau^{-\alpha}(\xi_{\parallel}\xi_{\perp}^2)_0\tau^{-3\nu},$$

$$= \alpha(\rho A^+/k_B)(\xi_{\parallel}\xi_{\perp}^2)_0, \quad (25)$$

where the final form follows from the hyperscaling relation $2-\alpha=3\nu$ that is valid for the 3D XY model. From Eqs. (13a) and (24), one obtains the universal expression $(R_{\xi}^+)^3 = \alpha X_1^C(X_1^{\xi})^3$, which yields the 3D XY theoretical value $R_{\xi}^+ = 0.3606 \pm 0.0020$ [19]. This value can be compared with experimental values of R_{ξ}^+ calculated from Eq. (25) using $\rho = 1.0 \text{ g cm}^{-3}$ as assumed earlier.

The experimental R_{ξ}^+ values are given in Table VI along with a summary of the θ_0 , A^+ , $(\xi_{\parallel}\xi_{\perp}^2)_0$, and σ_0 values used for our preasymptotic C_p and x-ray analysis. Agreement between theory and experiment is excellent for $T8$, DB_8ONO_2 and 8OPCBOB , good for $\text{DB}_5\text{CN} + \text{C}_5$ stilbene, and reasonably good for $T7$ in view of problems with the $T7$ heat-capacity data. It should be noted that the absolute value of $(\xi_{\parallel}\xi_{\perp}^2)_0$ depends somewhat on the choice of structure factor $S(\mathbf{q})$. The values of $(\xi_{\parallel}\xi_{\perp}^2)_0$ and R_{ξ}^+ in Table VI are based on use of the standard $S(\mathbf{q})$ form given in Eq. (1). Use of a Lorentzian $S(\mathbf{q})$ yields $(\xi_{\parallel}\xi_{\perp}^2)_0 \sim 2.9$ times larger and thus R_{ξ}^+ values ~ 1.4 times larger. Use of the power-law corrected Lorentzian $S(\mathbf{q})$ given by Eq. (3) in paper I yields $(\xi_{\parallel}\xi_{\perp}^2)_0 \sim 1.9$ times smaller and thus R_{ξ}^+ values ~ 1.2 times smaller. However, one must keep in mind the fact that the Lorentzian fits to the x-ray profiles are very poor [16], and Lorentzian $(\xi_{\parallel}\xi_{\perp}^2)_0$ values are therefore unreliable. The fits with Eq. (I-3) require empirical η_1 values that are less well behaved than the c values obtained with Eq. (1); thus we feel that

the smaller $(\xi_{\parallel}\xi_{\perp}^2)_0$ values obtained with Eq. (I-3) are also less reliable. One could take the view that universality arguments support the choice of the standard form for $S(\mathbf{q})$ or, more conservatively, the view that systematic errors in R_{ξ}^+ could be as large as ± 0.08 .

IV. DISCUSSION

In the past, it has been conventional to analyze N -Sm- A x-ray data using pure power laws for ξ_{\parallel} , ξ_{\perp} , and σ with effective nonuniversal critical exponents even when it was clearly established that the heat-capacity data for the system required corrections-to-scaling terms. This practice developed due to the fact that log-log plots of ξ_{\parallel} , ξ_{\perp} , and σ versus the reduced temperature τ did not show statistically significant curvature over 2.5–3 decades in τ . Furthermore, there was, and still is, no theory for the anisotropic critical behavior of ξ_{\parallel} and ξ_{\perp} to guide the choice of correction terms. In addition, the number of data points was usually too small for effective range-shrinking tests. Most x-ray data sets contain 20–40 data points over the $10^{-5} < \tau < 10^{-2}$ range, compared to several hundred C_p data points. Finally, the effective volume exponent $3\nu_{\text{eff}} = \nu_{\parallel} + 2\nu_{\perp}$ and the effective C_p exponent α_{eff} for N -Sm- A_m and N -Sm- A_d transitions seemed to obey hyperscaling ($\alpha_{\text{eff}} + 3\nu_{\text{eff}} = 2$) within the rather large (± 0.15) experimental uncertainties [7,8].

Recent investigations of several polar Sm- A_1 systems have established the following pattern: (1) C_p has a 3D XY form with $\alpha = \alpha_{XY} = -0.007$ and fairly large correction terms [13,14], (2) pure power-law values of ν_{\parallel} and ν_{\perp} do not conform to hyperscaling expectations, as described below, (3) the neglect of correction terms for $\xi_{\parallel}\xi_{\perp}^2$ and σ is inconsistent with theory in view of the large C_p correction terms that yield substantial values for θ_0 (see Fig. 5).

As an illustration of the failure of ν_{\parallel} and ν_{\perp} values obtained from pure power law as to satisfy hyperscaling, Fig. 9 shows a plot of ν_{\parallel} vs ν_{\perp} for N -Sm- A_1 systems with C_p data that are known to conform to 3D XY theory. One can write the anisotropic hyperscaling relation in the form $\nu_{\parallel} = 2 - \alpha - 2\nu_{\perp} = 2.0066 - 2\nu_{\perp}$. This locus of ν_{\parallel} , ν_{\perp} values that satisfy hyperscaling is shown as the dashed

TABLE VI. Nonuniversal parameters θ_0 , $(\xi_{\parallel}\xi_{\perp}^2)_0$, and σ_0 used to fit the x-ray data with preasymptotic 3D XY theory. The θ_0 values were held fixed at values obtained from an analysis of C_p data. Thus there is a single adjustable parameter for the correlation volume and another for the susceptibility. The universal ratio R_{ξ}^+ relating $(\xi_{\parallel}\xi_{\perp}^2)_0$ with the C_p amplitude A^+ is also given; its 3D XY value is 0.361 ± 0.002 . The uncertainties quoted in parentheses are 95% confidence limits associated with random errors, as determined from an F test.

System	θ_0	$-A^+ (JK^{-1}g^{-1})$	$(\xi_{\parallel}\xi_{\perp}^2)_0 (\text{\AA}^3)$	σ_0 (arb.)	R_{ξ}^+
$T8$	0.02(0.30)	3.34(0.20)	28.49(1.43)	0.254(0.012)	0.358(0.009)
$T7$	0.23(0.50)	1.93(0.24)	21.45(1.03)	0.281(0.011)	0.271(0.012)
DB_5CN	0.41(0.06)	18.59(0.23)	6.74(0.35)	0.825(0.035)	0.391(0.007)
+ C_5 stilbene					
DB_8ONO_2	0.48(0.11)	13.19(0.17)	7.07(0.37)	0.849(0.036)	0.355(0.006)
8OPCBOB	0.39(0.06)	31.45(0.41)	2.80(0.31)	0.316(0.030)	0.348(0.012)

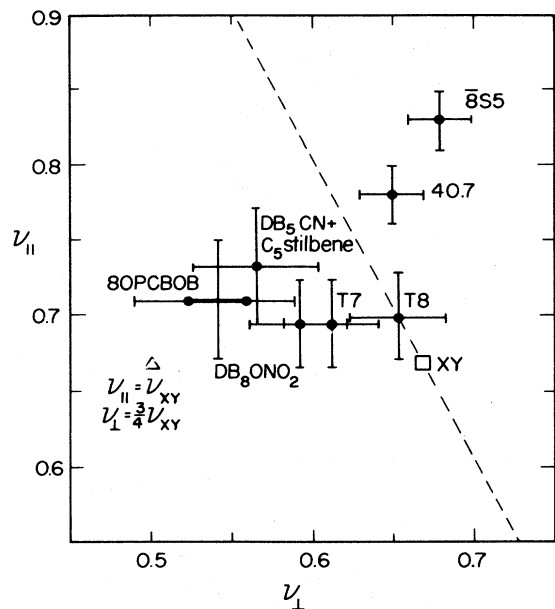


FIG. 9. Plot of ν_{\parallel} vs ν_{\perp} , where these effective exponents are obtained from pure power-law fits with Eq. (2). Standard deviations are indicated by the error bars. The dashed line gives the locus of $\nu_{\parallel}, \nu_{\perp}$ values that satisfy hyperscaling in systems with XY heat-capacity behavior ($\alpha = \alpha_{XY}$). The isotropic 3D XY point $\nu_{\parallel} = \nu_{\perp} = \nu_{XY}$ is indicated by the open square, and the Patton-Andereck regime [6] where $\nu_{\parallel} = \frac{4}{3}\nu_{\perp} = \nu_{XY}$ is indicated by the triangle. Data for the nonpolar $Sm-A_m$ compounds 40.7 and 8S5 are taken from Ref. [7].

line in Fig. 9. In addition to the isotropic 3D XY point and the XY hyperscaling line, we also plot the position of the effective $\nu_{\parallel}, \nu_{\perp}$ values predicted by Patton and Andereck [6] for an intermediate temperature regime where $\nu_{\parallel} = \nu_{XY}$ but $\nu_{\perp} = \frac{3}{4}\nu_{XY} = 0.502$. The Patton-Andereck calculation predicts an extended crossover from isotropic ($\nu_{\parallel} = \nu_{\perp} = \nu_{XY}$) to anisotropic ($\nu_{\parallel} = 2\nu_{\perp} = 2\nu_{XY}$) fixed points but does not consider the role of correction terms. In their model, coupling between the smectic-order parameter and nematic director fluctuations gives rise to the intermediate regime described above. The $N-Sm-A_1$ results given in Fig. 9 could be consistent with an evolution from very weak-coupling isotropic behavior for T8 toward this Patton-Andereck intermediate anisotropic regime. However, a quantitative calculation of the Patton-Andereck crossover function would be required to substantiate this idea.

Also shown in Fig. 9 are two nonpolar $N-Sm-A_m$ systems which have C_p behavior very close to XY theory. It should be noted that these two nonpolar systems with ~ 25 -K nematic ranges deviate from hyperscaling in a different manner than the $N-Sm-A_1$ systems and exhibit large γ values (~ 1.5) [7]. Indeed, it seems likely that there are two distinct classes of $\xi_{\parallel}, \xi_{\perp}$ and σ behavior in systems with XY -like heat-capacity behavior. For $N-Sm-A_1$ systems, ν_{\parallel} and γ are close to XY values but $\nu_{\perp} < \nu_{XY}$. For $N-Sm-A_m$ systems, ν_{\perp} is close to ν_{XY} but

$\nu_{\parallel} > \nu_{XY}$ and $\gamma \neq \gamma_{XY}$. It should be noted that for the splay elastic constant $K_1 = K_1^0 + \delta K_1$, the pretransitional excess δK_1 is large but nonsingular for nonpolar $Sm-A_m$ materials while δK_1 is close to zero for polar materials [31]. Since coupling between the smectic-order parameter and director splay deformations is a possible source of anisotropic behavior [3,6], it is not surprising that a difference in δK_1 would be reflected in the behavior of ξ_{\parallel} and ξ_{\perp} .

In view of the points discussed above and the fact that the $Sm A_1$ correlation volume $\xi_{\parallel}\xi_{\perp}^2$ can be well described with the 3D XY free energy F_{theor} determined only from C_p data (see Fig. 6), we believe that $\xi_{\parallel}\xi_{\perp}^2$ and σ should be described with preasymptotic 3D XY theory. Such fits must be restricted to the preasymptotic domain D_{preas} , over which higher-order correction terms can be neglected. The extent of D_{preas} is difficult to establish for $\xi_{\parallel}\xi_{\perp}^2$ and σ due to the sparse x-ray data. It can be estimated for the heat capacity [13], and for C_p a typical D_{preas} regime extends out to $\theta_0\tau \approx 2 \times 10^{-3}$.

An internally consistent analysis of ΔC_p , $\xi_{\parallel}\xi_{\perp}^2$, and σ shows that all of these properties can be well described by the exact preasymptotic theory of the isotropic 3D XY model [19,21]. Data fitting in the nematic phase has been achieved with a minimal set of adjustable parameters: four for ΔC_p (only two of which are independent parameters needed for the preasymptotic range) and one additional parameter for each of $\xi_{\parallel}\xi_{\perp}^2$ and σ . The essential nonuniversal parameters are given in Table VI. Figures 7 and 8 show that the scaled correlation volume and scaled susceptibility agree very well with 3D XY theory. Furthermore, the ratios A^-/A^+ , D_1^-/D_1^+ , R_B^+ , and the product R_{ξ}^+ are all in good agreement with universal 3D XY values; and, of course, hyperscaling is obeyed. Overall agreement between x-ray experiment and 3D XY theory is poorest for 8OPCBOB (see Tables IV and V), which may indicate some difficulty with the x-ray measurement or may be due to the fact that the nematic range is only 45 K in this case compared to ≥ 96 K in the other four systems.

The agreement between experimental and theoretical values for R_{ξ}^+ demonstrates the compatibility between the nonuniversal amplitudes for C_p and $\xi_{\parallel}\xi_{\perp}^2$. No such test exists for the amplitude of σ . It should be stressed that the agreement among values of R_{ξ}^+ is quite remarkable. Such agreement means that one can quantitatively predict, with no adjustable parameters, the behavior of $\xi_{\parallel}\xi_{\perp}^2$ over 6 decades in magnitude from a knowledge of experimental heat-capacity data and preasymptotic XY theory.

There are four major unresolved issues remaining: ξ_{\parallel} and ξ_{\perp} diverge differently in the N phase over the $10^{-5} < \tau < 10^{-2}$ range (see Ref. [6]); the correlation lengths measured directly with x rays and those determined indirectly from nematic elastic constant data agree quantitatively [7,32], in spite of predictions of gauge-dependent differences [3]; the C_p amplitude ratio A^-/A^+ agrees with the normal XY value and is inconsistent [13] with the theoretically expected [2] inverted- XY value; the behavior of the layer compression-

al elastic constant B in the Sm- A phase does not conform to the predictions of the de Gennes model [33]. These features may be related to problems of gauge dependence in the asymptotic limit [3], to very slow crossover between isotropic and anisotropic fixed points [6], or to the size of anisotropic correction terms that restrict the asymptotic regime to very small reduced temperatures (say $\tau < 10^{-6}$). The subtlety of N -Sm- A behavior is indicated by Monte Carlo simulations [34] on a lattice version of the de Gennes model that corresponds to the extreme type-II superconductor limit. Renormalization analysis in the superconducting gauge for such a model yields an isotropic critical point with an inverted C_p amplitude ratio [2,3]. However, the Monte Carlo numerical results show anisotropic critical behavior for ξ_{\parallel} and ξ_{\perp} ($\xi_{\parallel}/\xi_{\perp}$ calculated in the experimental x-ray gauge increases smoothly on cooling toward T_c) and no inversion of C_p amplitudes [34].

Further experimental x-ray work on systems exhibiting 3D XY heat-capacity behavior is in progress with a study of the N -Sm- A_2 transition in 7APCBB [35], which hopefully will help to clarify the generality of the behavior seen so far only in Sm- A_1 systems. A detailed syn-

chrotron x-ray study of the Sm- A_1 phase behavior below T_c would also be of value. In terms of theory, the most important initiatives would seem to be more precise Monte Carlo simulations and the development of a nonasymptotic model which allows one to assess the effects of anisotropy on the correction terms for ξ_{\parallel} and ξ_{\perp} . Our assumption that one can use isotropic 3D XY theory for σ and $\xi_{\parallel}\xi_{\perp}^2$ seems to be validated empirically but needs to be explored theoretically for a model that explains the differing behavior of the individual correlation lengths ξ_{\parallel} and ξ_{\perp} .

ACKNOWLEDGMENTS

The authors would like to thank H. T. Nguyen for providing samples of DB₅CN and C₅ stilbene, K. I. Blum for assistance with several technical experimental problems, and W. H. de Jeu for providing x-ray data for 8OPCBOB. We also wish to thank C. Dasgupta, D. L. Johnson, T. C. Lubensky, and J. P. Marcerou for stimulating discussions. This work was supported by National Science Foundation Grants Nos. DMR 90-07611 and DMR 90-22933.

*Present address: Francis Bitter National Magnet Laboratory, MIT, Cambridge, MA 02139.

- [1] P. G. DeGennes, *Solid State Commun.* **10**, 753 (1972); *Mol. Cryst. Liq. Cryst.* **21**, 49 (1973); *The Physics of Liquid Crystals* (Clarendon, Oxford, 1974).
- [2] B. I. Halperin, T. C. Lubensky, and S. K. Ma, *Phys. Rev. Lett.* **32**, 292 (1974); C. Dasgupta and B. I. Halperin, *ibid.* **47**, 1556 (1981).
- [3] T. C. Lubensky, *J. Chim. Phys.* **80**, 31 (1983), and references cited therein. This provides a review of renormalization calculations that is still relevant.
- [4] D. R. Nelson and J. Toner, *Phys. Rev. B* **24**, 363 (1981); J. Toner, *ibid.* **26**, 462 (1982).
- [5] J. Prost, *Adv. Phys.* **33**, 1 (1984); P. Barois, J. Pommier, and J. Prost, in *Solitons in Liquid Crystals*, edited by L. Lam and J. Prost (Springer-Verlag, Berlin, 1989).
- [6] B. R. Patton and B. S. Andereck, *Phys. Rev. Lett.* **69**, 1556 (1992).
- [7] D. L. Johnson, *J. Chim. Phys.* **80**, 45 (1983); C. W. Garland, M. Meichle, B. M. Ocko, A. R. Kortan, C. R. Safinya, J. J. Yu, J. D. Litster, and R. J. Birgeneau, *Phys. Rev. A* **27**, 3234 (1983), and references cited in each.
- [8] J. Thoen, H. Marynissen, and W. VanDael, *Phys. Rev. Lett.* **52**, 204 (1984); B. M. Ocko, R. J. Birgeneau, and J. D. Litster, *Z. Phys. B* **62**, 487 (1986).
- [9] K. J. Stine and C. W. Garland, *Phys. Rev. A* **39**, 3148 (1989).
- [10] L. Chen, J. D. Brock, J. Huang, and S. Kumar, *Phys. Rev. Lett.* **67**, 2037 (1991).
- [11] K. K. Chan, P. S. Pershan, L. B. Sorensen, and F. Hardouin, *Phys. Rev. A* **34**, 1420 (1986).
- [12] K. W. Evans-Lutterodt, J. W. Chung, B. M. Ocko, R. J. Birgeneau, C. Chiang, C. W. Garland, E. Chin, J. Goodby, and N. H. Tinh, *Phys. Rev. A* **36**, 1387 (1987).
- [13] C. W. Garland, G. Nounesis, and K. J. Stine, *Phys. Rev. A* **39**, 4919 (1989); C. W. Garland, G. Nounesis, K. J. Stine, and G. Heppke, *J. Phys. (Paris)* **50**, 2291 (1989).
- [14] G. Nounesis, C. W. Garland, and R. Shashidhar, *Phys. Rev. A* **43**, 1849 (1991); L. Wu, C. W. Garland, and S. Pfeiffer, *ibid.* **46**, 973 (1992).
- [15] W. G. Bouwman and W. H. de Jeu, *Phys. Rev. Lett.* **68**, 800 (1992); corrected data differing slightly from those published were provided by de Jeu and were used in our analysis.
- [16] G. Nounesis, K. I. Blum, M. J. Young, C. W. Garland, and R. J. Birgeneau, preceding paper, *Phys. Rev. E* **47**, 1910 (1993) denoted as paper I.
- [17] K. Ema, C. W. Garland, G. Sigaud, and N. H. Tinh, *Phys. Rev. A* **39**, 1369 (1989).
- [18] C. W. Garland, *Geometry and Thermodynamics: Incommensurate Crystals Liquid Crystals, and Quasicrystals*, edited by J.-C. Toledano, Vol. 229B of *Advanced Studies Institute, Series B* (Plenum, New York, 1990), pp. 221-254.
- [19] C. Bagnuls and C. Bervillier, *Phys. Rev. B* **32**, 7209 (1985); see also C. Bagnuls, C. Bervillier, D. I. Meiron, and B. G. Nickel, *ibid.* **35**, 3585 (1987).
- [20] C. Bervillier, *Phys. Rev. B* **34**, 8141 (1986).
- [21] C. Bagnuls and C. Bervillier, *Phys. Lett.* **112A**, 9 (1985).
- [22] G. Nounesis, M. J. Young, K. I. Blum, C. W. Garland, and R. J. Birgeneau, *Z. Phys. B* (to be published).
- [23] At lower temperatures, DB₅CN + C₅ stilbene exhibits the phase sequence Sm- A_1 -Sm- \bar{A} -Sm- A_{cren} -Sm- A_2 (Ref. [17]). For $T < 405$ K, scattering is observed at $(q_x, 0, q_0)$ in the Sm- \bar{A} phase and eventually at $(0, 0, q_0)$ in the Sm- A_2 phase. An x-ray study of this region is in progress and will be reported later.
- [24] At $t^* = \theta_0 \tau = 3 \times 10^{-3}$ (corresponding roughly to $\tau \approx 10^{-2}$), the percent error in Eq. (9) relative to Eq. (8) is -1.6% for C_p , 7.2% for χ , 8.3% for ξ , and thus 27% for

the correlation volume.

- [25] A. Aharony and G. Ahlers, *Phys. Rev. Lett.* **44**, 782 (1980).
- [26] Using Eq. (17) with g_{00} and $X_2^\xi X_3^\xi$ as adjustable parameters, one finds for ξ_\perp fits that the ratio $X_2^\xi X_3^\xi / 0.3754$ ranges from 1.5 to 10 except for 8OPCBOB where it is 32 400! For ξ_\parallel fits, this ratio ranges from -0.18 to -1.1 . We do not claim that such an *ad hoc* form is likely to represent the true theoretical expression. However, it should be kept in mind that a pure power law with nonuniversal exponent is merely another empirical two-parameter form without theoretical justification. Indeed, in neglecting explicit correction terms, one is assuming that a pure power law magically accounts for corrections-to-scaling via an effective exponent.
- [27] C. Gooden, R. Mahmood, D. Brisbin, A. Baldwin, D. L. Johnson, and M. E. Neubert, *Phys. Rev. Lett.* **54**, 1035 (1985).
- [28] D. Stauffer, M. Ferer, and M. Wortis, *Phys. Rev. Lett.* **29**, 345 (1972).
- [29] The value of Y for an isotropic 3D Ising system is found to be -0.11 both experimentally and theoretically.
- [30] A. J. Leadbetter, J. L. A. Durrant, and M. Rugman, *Mol. Cryst. Liq. Cryst.* **34**, 231 (1977); A. Zywockinski, S. A. Wieczorek, and J. Stecki, *Phys. Rev. A* **36** 1901 (1987).
- [31] D. L. Johnson (private communication).
- [32] S. Sprunt, L. Solomon, and J. D. Litster, *Phys. Rev. Lett.* **53**, 1923 (1984).
- [33] M. Benzekri, T. Claverie, J. P. Marcerou, and J. C. Rouillon, *Phys. Rev. Lett.* **68**, 2480 (1992); see also M. Benzekri, doctoral thesis, University of Bordeaux, 1990.
- [34] C. Dasgupta, *J. Phys. (Paris)* **48**, 957 (1987).
- [35] X. Wen, C. W. Garland, and G. Heppke, *Phys. Rev. A* **44**, 5064 (1991).